

# Calculation on diffraction aperture of cube corner retroreflector

Song Li (李松), Bei Tang (唐蓓), and Hui Zhou (周辉)

School of Electronic Information, Wuhan University, Wuhan 430079

Received April 8, 2008

On the basis of optical property of cube corner retroreflector (CCR), a new perception and calculation approach for diffraction aperture of CCR in two different forms is presented. The relationship between diffraction apertures and incident light with six different combinations of reflection order and incident angle is established. Far-field diffraction patterns of CCR under various incident conditions are also provided.

OCIS codes: 050.1220, 050.1940, 050.1960.

doi: 10.3788/COL20080611.0833.

Retroreflector has been widely used in various laser measurement systems as a cooperative target based on its direct reflecting<sup>[1,2]</sup>. Satellite laser ranging (SLR) which is a high-precision space measurement technology comes forth in the 1960s. The laser cooperation target in SLR system is laser cube corner retroreflector (CCR) or laser retroreflector array which is installed on the surface of the satellite. The orbital altitude of satellite is generally several hundred kilometers to tens of thousands of kilometers. Therefore, the SLR system can be regarded as a Fraunhofer diffraction optical system. On the one hand, CCRs on the satellite directionally reflect the laser pulse which comes from the observing station; on the other hand, CCRs diffract and redistribute energy of the laser pulse as diffraction aperture. The light field distribution diffracted by CCRs is of great significance for the laser ranging system to receive laser pulse echo correctly and to accomplish the ranging function exactly.

The most important parameter which influences the far-field diffraction characteristics of CCR is the integral region of diffraction aperture. However, previous researches into the far-field diffraction of CCR take the diffraction aperture as a whole. We want to explore the deeper reason what makes the light field distribution of CCR be taken on like that and why the certain part of light spot is much better than other parts of light spot for the reception. In this paper, the diffraction aperture theory of oblique incidence on the CCR is established.

The CCR consists of three mutually orthogonal planar surfaces and one flat bottom surface. The light which enters the CCR through the bottom surface is reflected by the three planar surfaces in turn. There are six different reflection orders of light as three reflective surfaces have six different sequences of arrangements<sup>[3]</sup>. The reflection order of light depends on the incident direction and coordinates of light on the bottom surface of CCR. Take the vertex of CCR as the origin and three edges of CCR as  $X$ ,  $Y$ ,  $Z$  axes to establish the coordinate system, as shown in Fig. 1. Without regard to refraction, for an incident light with any direction  $(a, b, c)$ , the light direction converts to  $(-a, -b, -c)$  after being reflected by the three reflective surfaces respectively.

As shown in Fig. 2, taking the midpoint of bottom sur-

face as the origin  $o$ , the bottom surface as  $x$ - $y$  plane, and the direction of light which comes out of the CCR after being reflected by the three reflective surfaces sequentially as  $z$ -axis, we establish the  $oxyz$  coordinate system. Draw a vertical line to one of the bottom surface borders across point  $O$  in  $X$ - $Z$  plane, with the foot of the perpendicular labeled as point  $T$ . It is assumed that the angle between line  $OT$  and  $z$ -axis is  $\varphi$ , and the angle between line  $OT$  and line  $Oo$  is  $\omega$ . These two sets of coordinates are provided with coordinate transformation matrix as<sup>[4]</sup>

$$\mathbf{M} = \begin{pmatrix} \cos \varphi & -\sin \varphi \sin \omega & -\sin \varphi \cos \omega \\ 0 & \cos \omega & -\sin \omega \\ \sin \varphi & \cos \varphi \sin \omega & \cos \varphi \cos \omega \end{pmatrix}. \quad (1)$$

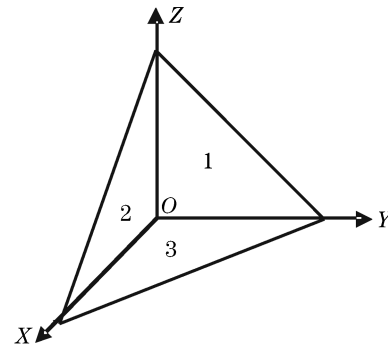


Fig. 1. Cartesian coordinates of CCR.

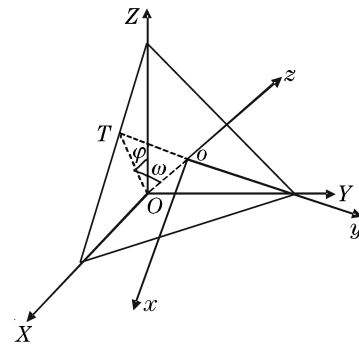


Fig. 2. Schematic diagram of coordinate transformation of CCR.

The coordinate transformations between  $OXYZ$  and  $oxyz$  coordinate systems go as

$$\begin{pmatrix} X \\ Y \\ Z \end{pmatrix} = \mathbf{M} \begin{pmatrix} x \\ y \\ z \end{pmatrix} + \begin{pmatrix} \frac{d}{3} \\ \frac{d}{3} \\ \frac{d}{3} \end{pmatrix}$$

$$= \begin{pmatrix} \frac{\sqrt{2}}{2} & -\frac{\sqrt{6}}{6} & \frac{\sqrt{3}}{3} \\ 0 & \frac{\sqrt{6}}{3} & \frac{\sqrt{3}}{3} \\ -\frac{\sqrt{2}}{2} & -\frac{\sqrt{6}}{6} & \frac{\sqrt{3}}{3} \end{pmatrix} \begin{pmatrix} x \\ y \\ z \end{pmatrix} + \begin{pmatrix} \frac{d}{3} \\ \frac{d}{3} \\ \frac{d}{3} \end{pmatrix}, \quad (2)$$

where  $d$  is defined as the right-angled edge length of the CCR.

Now we suppose that the unit vector of the incident light in the  $oxyz$  coordinate system is  $(-\sin\phi\cos\theta, -\sin\phi\sin\theta, -\cos\phi)$  just as shown in Fig. 3 and that in the  $OXYZ$  coordinate system is  $(-a_1, -a_2, -a_3)$ . The angle  $\phi$  of the unit vector is incident angle and the angle  $\theta$  is azimuth angle. These two sets of unit vector are tied up by the coordinate transformation matrix above. If taking account of refraction, we only need to multiply the unit vector by a certain factor. It is of the opinion that only lights which are incident on certain area of the bottom surface can be reflected respectively by those three right-angled planes (planes 1, 2, and 3) and come out through the bottom surface<sup>[5]</sup>. As mentioned above, there are six different reflection orders of light, which are  $1 \rightarrow 2 \rightarrow 3$ ,  $2 \rightarrow 1 \rightarrow 3$ ,  $3 \rightarrow 2 \rightarrow 1$ ,  $2 \rightarrow 3 \rightarrow 1$ ,  $3 \rightarrow 1 \rightarrow 2$ , and  $1 \rightarrow 3 \rightarrow 2$ . It is assumed that the intersecting points between light and planes 1, 2, and 3 are  $(0, Y_1, Z_1)$ ,  $(X_2, 0, Z_2)$ , and  $(X_3, Y_3, 0)$ , respectively, in the  $OXYZ$  coordinate system. It is assumed that light coming out from the CCR intersects the bottom surface at point  $(X, Y, Z)$  in the  $OXYZ$  coordinate system and point  $(x, y, z)$  in the  $oxyz$  coordinate system. Same as above, the incident light intersects the bottom surface of CCR at point  $(X', Y', Z')$  in the  $OXYZ$  coordinate system and point  $(x', y', z')$  in the  $oxyz$  coordinate system. As it has been figured out that six sets of reflection order match with six effective diffraction apertures correspondingly, we can get access to effective diffraction aperture of the CCR by fitting these six smaller apertures together<sup>[6]</sup>. We will take the reflection order of  $1 \rightarrow 2 \rightarrow 3$  as an example to illustrate how to calculate the effective diffraction aperture specifically.

Optical property of CCR that is mentioned above and

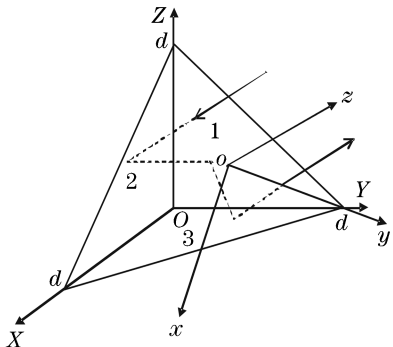


Fig. 3. Schematic diagram of light reflection by CCR.

knowledge about geometrical optics are applied to obtain a set of equation below:

$$\begin{cases} \frac{X-X_3}{a_1} = \frac{Y-Y_3}{a_2} = \frac{Z}{a_3} \\ X+Y+Z=d \end{cases}. \quad (3)$$

Solve Eq. (3), we get

$$\begin{cases} X = \frac{a_1 d - a_1 Y_3 + X_3(a_2 + a_3)}{a_1 + a_2 + a_3} \\ Y = \frac{a_2(d - X_3 - Y_3)}{a_1 + a_2 + a_3} + Y_3 \\ Z = \frac{a_3(d - X_3 - Y_3)}{a_1 + a_2 + a_3} \end{cases}. \quad (4)$$

One should notice that  $X, Y, Z$  are in the  $OXYZ$  coordinate system here, and the desired diffraction aperture is on the bottom surface of CCR. It is time to utilize the coordinate transformation matrix to make  $X, Y, Z$  convert to  $x, y, z$  in the  $oxyz$  coordinate system:

$$\begin{cases} x = \frac{\sqrt{2}}{2} \left[ \frac{(a_1 - a_3)d + X_3(a_2 + 2a_3) + (a_3 - a_1)Y_3}{a_1 + a_2 + a_3} \right] \\ y = \frac{\sqrt{6}}{6} \left[ \frac{-3a_2 X_3 + 3(a_1 + a_3)Y_3 + (2a_2 - a_1 - a_3)d}{a_1 + a_2 + a_3} \right] \\ z = 0 \end{cases}. \quad (5)$$

Regarding  $X_3$  and  $Y_3$  as attributive variables and  $x, y$  as independent variables in Eq. (5), then we get

$$\begin{cases} X_3 = \frac{\sqrt{2}}{2} \frac{a_3 + a_1}{a_3} x - \frac{\sqrt{6}}{6} \frac{a_3 - a_1}{a_3} y - \frac{1}{3} \frac{d(a_1 - a_3)}{a_3} \\ Y_3 = \frac{\sqrt{2}}{2} \frac{a_2}{a_3} x + \frac{\sqrt{6}}{6} \frac{a_2 + 2a_3}{a_3} y - \frac{1}{3} \frac{d(a_2 - a_3)}{a_3} \end{cases}. \quad (6)$$

Furthermore, we get the relational expressions of  $(X_3, Y_3, 0)$  with  $(0, Y_1, Z_1)$  and  $(X_2, 0, Z_2)$ :

$$\begin{cases} X_2 = X_3 - \frac{a_1 Y_3}{a_2} \\ Y_2 = 0 \\ Z_2 = \frac{a_3 Y_3}{a_2} \end{cases}, \quad \begin{cases} X_1 = 0 \\ Y_1 = \frac{a_2}{a_1} X_3 - Y_3 \\ Z_1 = \frac{a_3}{a_1} X_3 \end{cases}. \quad (7)$$

Same as above, we get the relational expression of  $(x', y', z')$  with  $(0, Y_1, Z_1)$ :

$$\begin{cases} x' = \frac{\sqrt{2}}{2} \left[ \frac{(a_1 - a_3)d + (a_3 - a_1)Y_1 - (2a_1 + a_2)Z_1}{a_1 + a_2 + a_3} \right] \\ y' = \frac{\sqrt{6}}{6} \left[ \frac{3(a_1 + a_3)Y_1 - 3a_2 Z_1 + (2a_2 - a_1 - a_3)d}{a_1 + a_2 + a_3} \right] \\ z' = 0 \end{cases}. \quad (8)$$

The area coverage of  $(x, y, 0)$  which meets the constraints of  $\begin{cases} Y_1 \geq 0 \\ Z_1 \geq 0 \end{cases}$ ,  $\begin{cases} X_2 \geq 0 \\ Z_2 \geq 0 \end{cases}$ ,  $\begin{cases} X_3 \geq 0 \\ Y_3 \geq 0 \end{cases}$  represents the effective diffraction aperture which goes with the reflection order of  $1 \rightarrow 2 \rightarrow 3$ . We should also pay attention to the confinement of the CCR's bottom shape on  $(x, y, z)$  and  $(x', y', z')$ . As shown in Fig. 4, they are the effective diffraction apertures of reflection

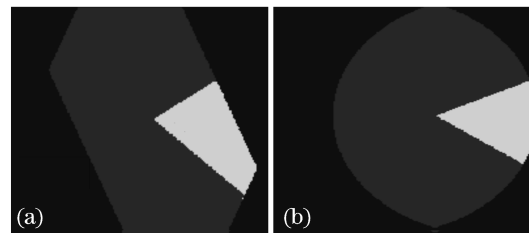


Fig. 4. Effective diffraction aperture of the reflection order  $1 \rightarrow 2 \rightarrow 3$ . (a) Triangular bottom with incident angle of  $15^\circ$ ; (b) circular bottom with incident angle of  $20^\circ$ .

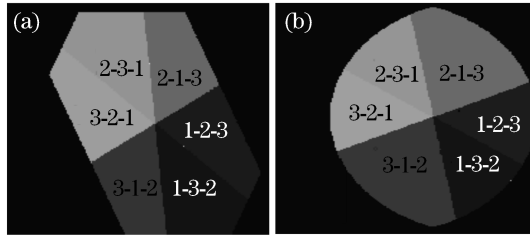


Fig. 5. Effective diffraction aperture of CCR. (a) Triangular bottom with incident angle of  $15^\circ$ ; (b) circular bottom with incident angle of  $20^\circ$ .

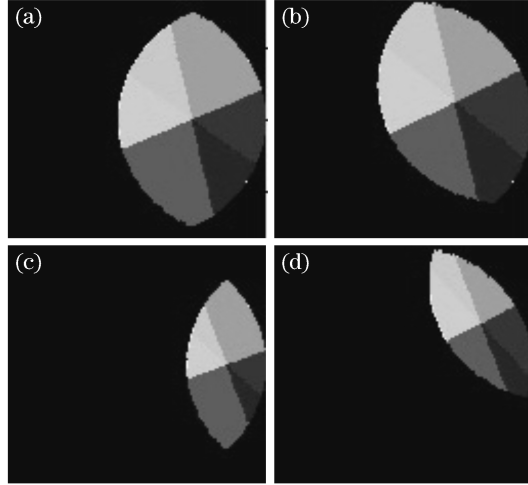


Fig. 6. Effective diffraction aperture of CCR with circular bottom for different values of incident angle  $\phi$  and azimuth angle  $\theta$ . (a)  $\phi = 25^\circ$ ,  $\theta = 0^\circ$ ; (b)  $\phi = 25^\circ$ ,  $\theta = 20^\circ$ ; (c)  $\phi = 40^\circ$ ,  $\theta = 0^\circ$ ; (d)  $\phi = 40^\circ$ ,  $\theta = 30^\circ$ .

order  $1 \rightarrow 2 \rightarrow 3$  coming along with triangular bottom and circular bottom respectively. Calculating other five effective diffraction apertures and combining these six apertures together, we obtain the effective diffraction aperture of CCR, which is presented in Fig. 5.

The above method is applied to get several pictures of effective diffraction aperture which differ in the incident angle and azimuth angle. From Fig. 6, it is worth noticing that the area of effective diffraction aperture does not change with the azimuth angle which only affects the position of diffraction aperture. The effective diffraction aperture rotates an angle of  $\theta$  compared with the diffraction aperture with azimuth angle  $0^\circ$ , so the azimuth angle will have effect on the intensity distribution of CCR's far-field diffraction.

The area of diffraction aperture decreases as the incident angle increases, as shown in Fig. 7. The effective diffraction aperture decreases to zero when the incident angle comes to a threshold value. The transformation rules for the six diffraction apertures coming from six reflection orders of incident light are not identical, but thanks to symmetrical characteristics, there are three groups of transformation rules. Reflection orders  $1 \rightarrow 2 \rightarrow 3$  and  $3 \rightarrow 2 \rightarrow 1$  have the same transformation rule in diffraction aperture, so do  $1 \rightarrow 3 \rightarrow 2$  and  $2 \rightarrow 3 \rightarrow 1$ ,  $3 \rightarrow 1 \rightarrow 2$  and  $2 \rightarrow 1 \rightarrow 3$ . Three different variation curves of diffraction aperture changing with incident angle are presented in Fig. 7, in which the diffraction apertures are normalized by the effective

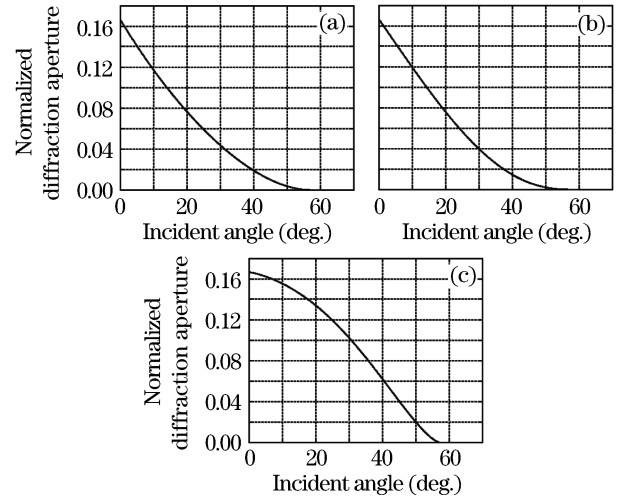


Fig. 7. Diffraction aperture variation curves with different reflection orders. (a) Reflection order  $1 \rightarrow 2 \rightarrow 3$ ; (b)  $1 \rightarrow 3 \rightarrow 2$ ; (c)  $3 \rightarrow 1 \rightarrow 2$ .

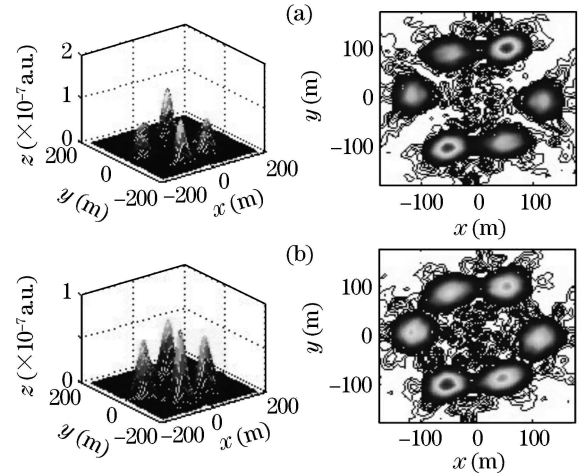


Fig. 8. Far-field diffraction pattern of CCR with the incident angle of  $15^\circ$  and azimuth angles of (a)  $0^\circ$  and (b)  $20^\circ$ . The  $z$  axis gives the relative energy magnitude.

diffraction aperture when the incident angle of light is zero.

From Fig. 7, we can find that the variation curves of diffraction aperture for the reflection orders  $1 \rightarrow 2 \rightarrow 3$  and  $1 \rightarrow 3 \rightarrow 2$  are much more similar compared with the variation curve for the reflection order  $3 \rightarrow 1 \rightarrow 2$ . The decreasing rate of variation curve in Fig. 7(c) ( $3 \rightarrow 1 \rightarrow 2$ ) is smoother than the other two as the incident angle of light increases. The six diffraction apertures with six reflection orders are equal when the incident angle of light is zero, and they reduce to zero at the same time when the incident angle of light increases to a certain degree. In general, light spot reflected back from the CCR on the satellite is too large to be received completely by the receiving telescope on the observing station<sup>[7,8]</sup>. That is to say, most energy of light reflected back has to be wasted due to the limited size of the receiving telescope. Under the best conditions, the telescope receives the part of light spot of which energy density is relatively high. From Fig. 7, it can be easily found that the proportion of diffraction aperture with reflection order  $3 \rightarrow 1 \rightarrow 2$  is larger than the other two when the in-

cident angle is not zero, and the diffraction aperture in this case changes more slowly than the other two. For this reason, the part of light spot which corresponds to the reflection order  $3 \rightarrow 1 \rightarrow 2$  or  $2 \rightarrow 1 \rightarrow 3$  is more preferable for the receiving telescope to detect. This can be further verified by the far-field diffraction patterns of CCR shown in Fig. 8.

Effective diffraction aperture and computational formula of diffraction presented in Ref. [9] are used to acquire the far-field diffraction pattern of CCR which is 960 km away from the observing station on the Earth and of which certain velocity aberration of light is offset. Figure 8 shows the patterns corresponding to incident angle  $15^\circ$  with azimuth angles of  $0^\circ$  and  $20^\circ$ . The relative energy magnitude is given with the projectile energy on cube corner retroreflector assumed to be a unit value. From Fig. 8, we can arrive at that the far-field diffraction pattern changes with the effective diffraction apertures because the effective diffraction aperture varies with incident angle and azimuth angle. We usually calculate the laser energy arriving at the receiving telescope in an approximate way that assumes the energy to be in direct proportion to the specular cross section of CCR<sup>[10]</sup>. But that is not the case, the receiving energy of different parts in the light spot is different, even the energy of the same part is changing with the incident angle and azimuth angle. We can find the optimum point for receiving telescope by applying the approach proposed in this paper.

We have provided the calculation method of CCR's diffraction aperture with different incidence condition

and with different reflection order of light. The diffraction aperture has an influence on the far-field diffraction pattern of CCR and also on the reception part of SLR system. The results in this paper are of importance in the designing of CCR.

S. Li's e-mail address is yflisong@public.wh.hb.cn.

## References

1. Z. Zhang, Z. Cheng, Z. Qin, and J. Zhu, Chinese J. Lasers (in Chinese) **34**, 694 (2007).
2. H. Chen, X. Ding, Z. Zhong, Z. Xie, and H. Yue, Acta Opt. Sin. (in Chinese) **27**, 1027 (2007).
3. Q. Wan, Y. Guo, X. Wang, B. Sun, C. Lu, and S. Wei, Laser Optoelectron. Prog. (in Chinese) **42**, (5) 20 (2005).
4. H. Nie, X. Weng, S. Li, and J. Liu, Acta Opt. Sin. (in Chinese) **23**, 1470 (2003).
5. Y. Cai, Z. Fang, G. Chen, and G. T. Chen, Chinese J. Lasers B **9**, 429 (2000).
6. H. Chen and J. Tan, J. Optoelectron. Laser (in Chinese) **17**, 986 (2006).
7. J. J. Degnan, "Millimeter accuracy satellite laser ranging: A review" in *Contributions of Space Geodesy to Geodynamics Technology, Geodynamics Series, Vol.25* (American Geophysical Union, Washington, 1993) pp.133–162.
8. R. Neubert, in *Proceedings of 10th Workshop on Laser Ranging Instrumentation* 216 (1996).
9. H. Zhou, S. Li, Y. Shi, X. Weng, and K. Hu, Opto-Electronic Eng. (in Chinese) **32**, (11) 25 (2005).
10. Y. Wang, F. Yang, and W. Chen, Opto-Electronic Eng. (in Chinese) **34**, (10) 25 (2007).